J. Biochem. **129**, 537–542 (2001)

Isolation and Characterization of an *N*-Linked Oligosaccharide That Is Significantly Increased in Sera from Patients with Non–Small Cell Lung Cancer[1]

Yosuke Otake,*,† Ichiro Fujimoto,* Fumihiro Tanaka,† Tatsuo Nakagawa,† Takeshi Ikeda,* Krishna K. Menon,* Sumihiro Hase,‡ Hiromi Wada,† and Kazuhiro Ikenaka*,[2]

Laboratory of Neural Information, National Institute for Physiological Sciences, 38 Myodaiji-cho Nishigonaka, Okazaki 444-8585; †Department of Thoracic Surgery, Faculty of Medicine, Kyoto University, 53 Shogoin Kawahara-cho, Sakyo-ku, Kyoto 606-8507; and ‡Department of Chemistry, Graduate School of Science, Osaka University, 1-1 Machikaneyama-cho, Toyonaka, Osaka 560-0043

Received October 18, 2000; accepted January 16, 2001

The structures of *N*-linked oligosaccharides present in human sera from 12 healthy volunteers and from 14 patients with non-small cell lung cancer (NSCLC) were analyzed by our recently developed partially automated systematic method. Thirty different structures of oligosaccharides were deduced, and these accounted for 84.1% of the total *N*-linked oligosaccharides present in human sera. All of the quantified oligosaccharide levels in healthy human sera were within twice the standard deviation. The amount of a triantennary trigalactosylated structure with one outer arm fucosylation (A3G3Fo) was found to be markedly increased in NSCLC patients in comparison to that in healthy volunteers ($p < 0.01$). No significant positive correlation with other clinical data was found. Serum A3G3Fo levels can thus be a novel marker for the diagnosis of NSCLC.

Key words: high performance liquid chromatography, *N*-linked oligosaccharide, non-small cell lung cancer, serum, two-dimensional map.

Non–small cell lung cancer (NSCLC) is an ordinary solid tumor with poor prognosis: the 5-year survival rate of patients with NSCLC after surgical resection has remained at only 20–35% (*1*). Even with the recent advances in cancer diagnostic methodology, the incidence of NSCLC worldwide has increased progressively (*2*). The poor prognosis is attributable to the difficulty of early detection and a high recurrence rate during post-operative observation periods, due at least in part to the lack of reliable tumor markers against NSCLC. Here we report that the amount of one *N*-linked oligosaccharide is significantly increased in the sera of patients with NSCLC.

We have recently developed a partially automated systematic method for analyzing *N*-linked oligosaccharide patterns present in whole tissue without purification of the glycoproteins (*3*). Using this method, *N*-linked oligosaccharides were detectable from amounts as low as 1 to 2 mg of acetone-precipitated tissues or sera. We have already demonstrated that patterns of *N*-linked oligosaccharides present in identical regions of age-matched mouse or human brains as well as those in human sera are extremely similar, which indicates that the expression patterns of *N*-linked oligosaccharides are strictly controlled. Hence, the applicability of this method to clinical diagnosis was implicated. In this study we applied this method to analyze *N*-linked oligosaccharides in sera from NSCLC patients.

MATERIALS AND METHODS

Preparation of Serum Samples—Fasting peripheral blood was collected from 12 healthy volunteers (7 males and 5 females; mean age, 30.2) as controls and 14 patients (11 males and 3 females; mean age, 64.5) with NSCLC including 5 adenocarcinomas, 5 squamous cell carcinomas and 4 large cell carcinomas. These diagnoses were based on the WHO classification (*4*), and their clinical stages were based on the TNM classification as revised in 1997 (*5*) in Kyoto University Hospital. Informed consent was obtained from all patients. A 9-fold volume of acetone was added to approximately 100 μl of the collected serum samples, which were centrifuged at 10,000 ×*g* for 20 min at 4°C, and the resulting pellet was dried in a vacuum centrifuge.

Preparation and Analysis of Pyridylaminated Oligosaccharides—We have previously described methods to prepare pyridylaminated (PA-) oligosaccharides by GlycoPrep™ 1000 (Oxford GlycoSystems, Oxford, UK) and GlycoTag™ (Takara, Tokyo), and to treat them with neuraminidase (from *Arthrobacter ureafaciens*, Nacalai Tesque, Kyoto) (*3*). Size-fractionation HPLC and reversed-phase HPLC were carried out essentially in the same manner as reported previously (*3*). We modified the reversed-phase HPLC method by adding compounds of known glucose unit

[1] This research was supported in part by Grants-in-Aid 10878144 (to K.I.) and 11671317 (to F.T.) for Scientific Research from the Ministry of Education, Science, Sports and Culture of Japan.

[2] To whom correspondence should be addressed. Tel: +81-564-55-7841, Fax: +81-564-55-7843. E-mail: ikenaka@nips.ac.jp

[3] The nomenclature of oligosaccharide structures is as follows: A*n* (where n = 2–4) indicates the number of antennae linked to the trimannosyl core; G*n* (where n = 0–4), the number of galactose residues attached to the non-reducing ends; F, with core fucosylation; Fo, with outer arm fucosylation attached α1-3 to *N*-acetylglucosamine; B, with bisecting *N*-acetylglucosamine.

© 2001 by The Japanese Biochemical Society.

Downloaded from http://jb.oxfordjournals.org/ at Peking University on October 1, 2012

(GU) value as internal standards. Before applying the serum sample, PA-glucose oligomer (Takara), consisting of pyridylaminated isomaltooligosaccharides containing PA-labeled glucose trimer to 22-mer, was injected onto the column. The GU value of each sample peak was calculated by comparing its elution time with those of the two nearest peaks of glucose oligomers. Power Chrom™ system (AD Instruments, NSW, Australia) with a Macintosh™ computer (Apple Computer, Cupertino, CA, USA) was used for analysis of area and elution times for each peak.

Preparation of Two-Dimensional Map for Standard Oligosaccharides—Various structures of standard oligosaccharides with or without PA label were purchased from Takara, Seikagaku Corporation (Tokyo), or Oxford GlycoSystems. The nomenclature of oligosaccharide structure is shown in footnote 3.[3] Standard oligosaccharides without PA derivatization were applied to GlycoTag™ to be labeled by pyridylamination. PA-standard oligosaccharides were injected to both size-fractionation and reversed-phase HPLC in the same manner as described above. The GU value of each standard oligosaccharide was also calculated as described above, and their mannose unit (MU) values were calculated from the elution times of the two nearest oligomannose series standard oligosaccharides. The M10 elution time was settled as M9 elution time + 1.5 min. We thus obtained a two-dimensional map for standard oligosaccharides by using the two indexes of MU and GU values (Fig. 1).

Determination of the Structure of Sample Oligosaccharides—The most abundant 100 peaks after reversed-phase HPLC were collected from four samples: two healthy volunteers and two NSCLC patients. Each collected peak sample was re-applied to size-fractionation HPLC and its MU values were calculated. A point determined from GU and MU values for each peak of reversed-phase HPLC was plotted on the two-dimensional map for standard oligosaccharides. We determined the oligosaccharide structure represented by collected peaks by comparing their positions in the two-dimensional map against standard oligosaccharides. When the same structure was detected in two or more fractions, the summation of each area of the same structure was used as the content of the structure. The content was expressed as the molar percentage of the total *N*-linked oligosaccharides contained in the serum.

Enzyme Digestion—All the enzymes were obtained from Boeringer Mannheim (Tokyo). Oligosaccharides were digested with α-L-fucosidase (from beef kidney; 1 mU) in 50 mM sodium acetate buffer, pH 6.0, at 37°C for 10 min, β-galactosidase (from *Diplococcus pneumoniae*; 1 mU) in 50 mM sodium acetate buffer, pH 6.0, at 37°C for 60 min or *N*-acetyl-β-D-glucosaminidase (from *D. pneumoniae*; 12 mU) in 50 mM sodium acetate buffer, pH 5.0, at 37°C for 24 h.

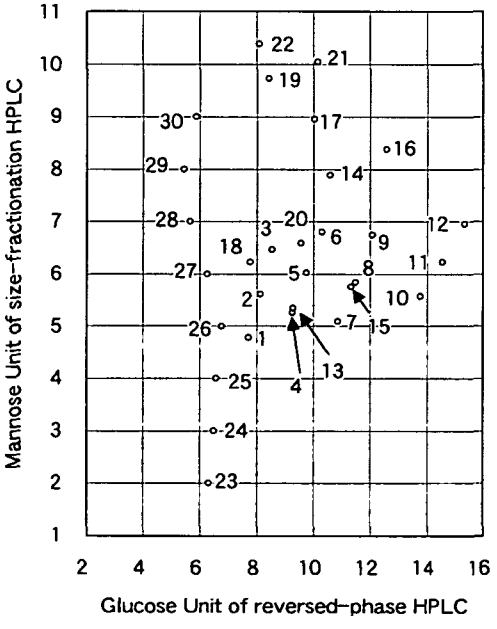

Fig. 1. **Two-dimensional map for standard oligosaccharides.** The abscissa indicates mannose unit values calculated from the elution time on size-fractionation HPLC, and the ordinate glucose unit values from reversed-phase HPLC. The numbers of the plotted points indicate the following oligosaccharide structures: 1, A2G0; 2, A2G1; 3, A2G2; 4, A2G0F; 5, A2G1F; 6, A2G2F; 7, A2G0B; 8, A2G1B; 9, A2G2B; 10, A2G0FB; 11, A2G1FB; 12, A2G2FB; 13, A3G0; 14, A3G3; 15, A3G0F; 16, A3G3F; 17, A3G3Fo; 18, A4G0; 19, A4G4; 20, A4G0F; 21, A4G4F; 22, A4G4Fo; 23, M2B; 24, M3; 25, M4B; 26, M5A; 27, M6B; 28, M7A; 29, M8A; 30, M9A. The nomenclature of the structures is shown in footnote 3.[3]

RESULTS

Expression Pattern of Asialo N-Linked Oligosaccharides in Human Sera of Healthy Volunteers and Prediction of the Structures—The amounts of asialo *N*-linked oligosaccharides expressed in human sera of healthy volunteers are listed in the left column of Table I. Representative HPLC elution profiles and their structures are shown in Fig. 2A. We have identified the *N*-linked oligosaccharide structures of 84.1% of total *N*-linked oligosaccharides expressed in human sera as described in "MATERIALS AND METHODS."

TABLE I. ***N*-linked oligosaccharide content expressed in human sera of healthy volunteers and NSCLC patients.**

Structure[a] (No.[b])	Content ratio (mean ± SD%)	
	Healthy volunteers (n = 12)	NSCLC patients (n = 14)
Biantennary		
A2G0 (1)	0.24 ± 0.04	0.29 ± 0.13
A2G1 (2)	1.18 ± 0.36	0.73 ± 0.30
A2G2 (3)	40.18 ± 4.03	39.88 ± 6.89
A2G0F (4)	3.91 ± 1.19	5.68 ± 1.99
A2G1F (5)	7.11 ± 1.65	5.47 ± 1.43
A2G2F (6)	13.70 ± 3.46	10.33 ± 3.14
A2G0FB (10)	1.12 ± 0.47	1.21 ± 0.43
A2G1FB (11)	1.17 ± 0.49	1.16 ± 0.54
A2G2FB (12)	2.37 ± 0.58	2.45 ± 0.85
Triantennary		
A3G3 (14)	6.81 ± 2.66	6.72 ± 2.57
A3G3F (16)	0.37 ± 0.12	0.29 ± 0.15
A3G3Fo* (17)	1.91 ± 1.09	4.78 ± 2.79
Tetraantennary		
A4G4 (19)	2.17 ± 0.88	1.92 ± 0.58
A4G4Fo (22)	0.18 ± 0.32	0.26 ± 0.15
Oligomannose series		
M5A (26)	0.85 ± 0.15	1.34 ± 1.60
M6B (27)	0.17 ± 0.05	0.18 ± 0.04
M8A (29)	0.29 ± 0.13	0.18 ± 0.05
M9A (30)	0.59 ± 0.18	0.51 ± 0.15

[a]The nomenclature of oligosaccharide structure is shown in footnote 3. [b]Numbers in parentheses correspond to those in Figs. 1 and 2. *$p < 0.01$ (Student's test with 2 tails).

Downloaded from http://jb.oxfordjournals.org/ at Peking University on October 1, 2012

When the number of antennae was considered, biantennary structures were expressed most abundantly and accounted for 70.9% of all *N*-linked oligosaccharides. Tri- and tetraantennary structures accounted for 9.1 and 2.3%, respectively. In an oligomannose series, the M5A and M9A structures were the major components, but constituted less than 1% of the entire *N*-linked oligosaccharide population. Among the *N*-linked oligosaccharides present in sera, A2G2 structure was the most abundant, accounting for 40.1% of all *N*-linked oligosaccharides, followed by A2G2F and A3G3 structures. The amounts of *N*-linked oligosaccharides exceeding 1% of the total amount did not vary significantly among the samples, and all their values were distributed within twice the standard deviation (SD). This indicates that the expression of *N*-linked oligosaccharides is strictly controlled in human sera.

N-Linked Oligosaccharide Structures Significantly Increased in NSCLC Patients—The amounts of asialo *N*-linked oligosaccharides in NSCLC patients are listed in the right column of Table I, and statistically compared to those of healthy volunteers. The structures constituting 1% or less of total *N*-linked oligosaccharides were excluded from statistical analysis because the values were too small to be estimated correctly. Representative HPLC elution profiles and their structures are shown in Fig. 2B. At a statistical difference level of $p < 0.01$, the amount of peak 17 (Figs. 1 and 2) in NSCLC patients was significantly higher than in healthy volunteers, being more than two times greater. The coordinate of this peak on the two-dimensional map was very close or identical to that of A3G3Fo. This structure was determined as described below and is shown in Fig. 3. Its distributions in both groups are shown in Fig. 4.

Determination of the Structure of Oligosaccharide Whose Level Was Elevated in NSCLC Patient Sera—The structure of the oligosaccharide whose level was elevated in NSCLC patient sera (peak 17 in Figs. 1 and 2) was determined as follows. The oligosaccharide was coinjected with commercially available standard oligosaccharides onto the size-fractionation HPLC column and was shown to coelute with A3G3Fo. It was then digested with α-L-fucosidase, digesting both α1→3 and α1→4 linkages, followed by β-galactosi-

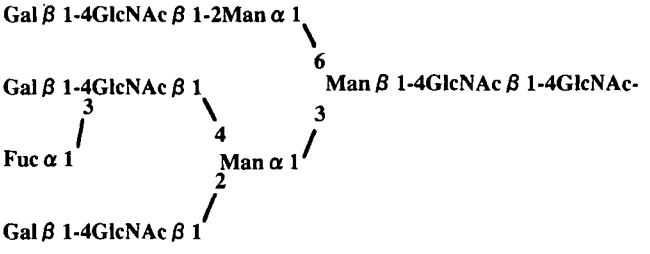

Fig. 3. **Structure of A3G3Fo.** GlcNAc indicates *N*-acetylglucosamine; Man, mannose; Gal, galactose; Fuc, fucose.

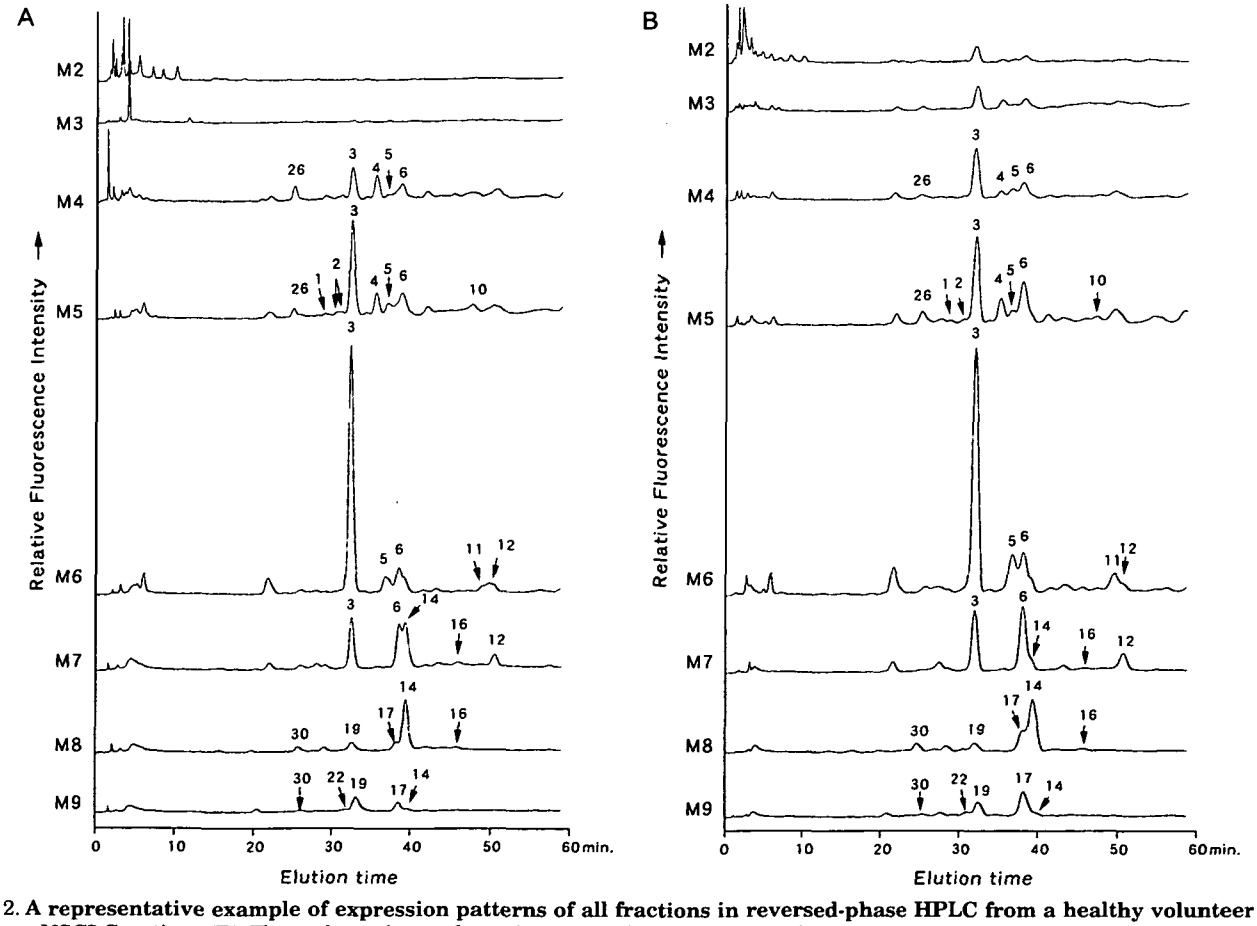

Fig. 2. **A representative example of expression patterns of all fractions in reversed-phase HPLC from a healthy volunteer (A) and an NSCLC patient (B).** The peak numbers refer to the oligosaccharide structures in Fig. 1.

Downloaded from http://jb.oxfordjournals.org/ at Peking University on October 1, 2012

dase, which selectively cleaves β1→4 but not β1→3 linkages. The digested oligosaccharide coeluted with A3G0, indicating that all the galactose residues were connected *via* β1→4 linkages. This strongly suggests that the fucose residue had been connected *via* an α1→3 linkage. Next, the oligosaccharide was first digested with β-galactosidase. The elution profile from size-fractionation HPLC suggested that two galactose residues had been removed. This indicated that the galactose residue on the branch with the fucose residue was resistant to the β-galactosidase digestion. The resulting oligosaccharide was further digested with *N*-acetyl-β-D-glucosaminidase, purified, and digested with α-L-fucosidase followed by β-galactosidase. The product contained one GlcNAc residue attached to a trimannosyl core. All three possible products (GlcNAc attached to mannose residue on α1→6 branch, and both β1→4 and β1→2–linked GlcNAc on α1→3–linked mannose residue) were available as standards, and their elution times on the reversed phase HPLC were significantly different from one another. The digested product coeluted with:

GlcNAcβ1→4Manα1→3, (Manα1→6)Manβ1→
4GlcNAcβ1→4GlcNAc-PA

Thus the structure of the peak 17 oligosaccharide was deduced to be A3G3Fo as shown in Fig. 3.

Correlation of A3G3Fo Level with Other Clinical Data— The possible correlation of serum A3G3Fo levels with other clinical data of NSCLC patients was investigated (Table II). In this study we only investigated neutral *N*-linked oligosaccharides after removal of sialic acid. Therefore a portion of A3G3Fo structures may have contained sialyl Lewis X (SLX) epitopes in their structures before neuraminidase-treatment. Serum SLX value has been demonstrated to be

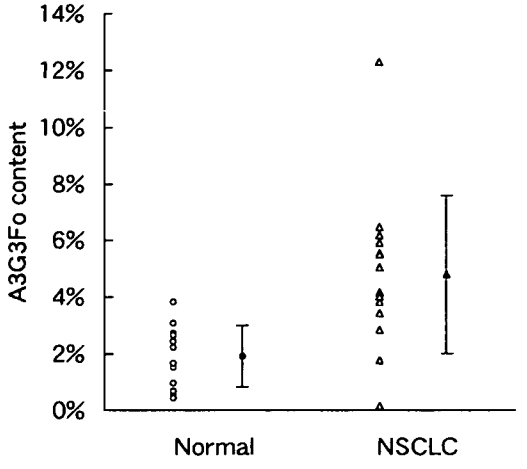

Fig. 4. **Proportions of A3G3Fo relative to total *N*-linked oligosaccharides expressed in sera from healthy volunteers and NSCLC patients.** Open circles (○) indicate the distribution of the sample from healthy volunteers, open triangles (△) from NSCLC patients. Closed circles (●) and triangles (▲) indicate mean value of healthy volunteers and NSCLC respectively, and their error bars indicate the standard deviations. Statistical differences were found at $p < 0.01$.

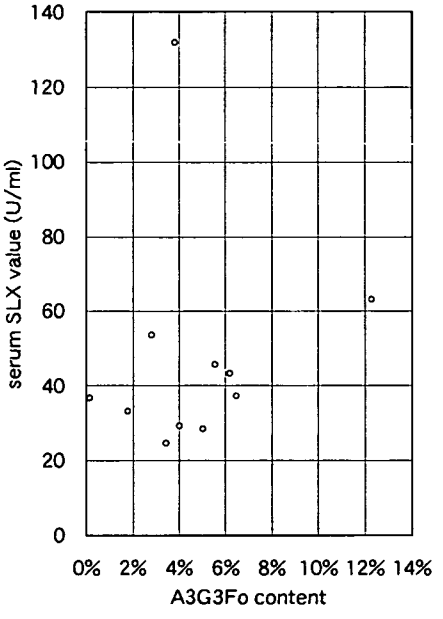

Fig. 5. **Relationship of serum A3G3Fo content and serum SLX value in NSCLC patients.** There is no significant correlation among them (correlation coefficient: 0.0197).

TABLE II. **The state of the disease, A3G3Fo content, serum SLX value, inflammatory reactions, and liver function of NSCLC patients.**

Case No.	Path[a]	Clinical stage[b]	A3G3Fo (%)[c]	SLX[d] (U/ml)	WBC[e] (/mm³)	CRP[f] (μg/ml)	GOT[g] (IU/liter)	GPT[h] (IU/liter)
1	Adeno	I	0.15	36.9	4300	<0.1	14	8
2	Adeno	IIIb	4.01	29.4	10900	0.6	11	5
3	Adeno	IV	5.91	ND[i]	ND	ND	ND	ND
4	Adeno	IV	3.82	132.0	9300	0.2	16	9
5	Adeno	IV	2.83	53.7	6100	0.1	35	16
6	SqCC	I	4.15	ND	5100	0.2	21	16
7	SqCC	I	3.43	24.7	9300	1.3	21	24
8	SqCC	I	5.03	28.6	5500	<0.1	16	11
9	SqCC	II	5.48	ND	5000	0.2	ND	ND
10	SqCC	IV	6.17	43.4	ND	ND	18	14
11	Large	I	5.54	45.8	4300	0.3	26	18
12	Large	I	1.77	33.3	5900	0.1	26	33
13	Large	II	12.28	63.2	7700	6.3	37	26
14	Large	IIIa	6.46	37.4	9800	0.6	23	25

[a]Pathological diagnosis, Adeno; adenocarcinoma, SqCC; squamous cell carcinoma, Large; large cell carcinoma. [b]Clinical stage of the disease. [c]The proportion of A3G3Fo structure expressed in total serum *N*-linked oligosaccharides. [d]Sialyl Lewis X. [e]White blood cell count (R^2 = 0.0456 *vs.* A3G3Fo). [f]C-reactive protein (R^2 = 0.6780 *vs.* A3G3Fo). [g]Glutamic oxaloacetic transaminase. [h]Glutamic pyruvic transaminase. [i]Not determined.

Downloaded from http://jb.oxfordjournals.org/ at Peking University on October 1, 2012

a good marker for the detection of cancers (*6*); thus levels of serum SLX antigen were also measured in 11 out of the 14 samples from patients with NSCLC. Five of the 11 samples (45.4%) surpassed the SLX cut-off value (37 U/ml). However, the A3G3Fo level exceeded the 2SD value in only 3 out of the 5 samples, and the samples with high SLX value did not always exhibit high A3G3Fo levels (Table II). Hence, only a weak positive correlation was observed between serum SLX value and the A3G3Fo structure content (Fig. 5). The A3G3Fo level can thus serve as an indicator of NSCLC independently of the SLX value. We have not excluded the possibility that up-regulated serum A3G3Fo levels in NSCLC patients is caused by a factor unrelated to malignancy. However, measurement of white blood cell count (WBC) or C-reactive protein level (CRP) indicated that the inflammatory reaction and A3G3Fo levels have little correlation (Table II). It was reported that the oligosaccharide structures attached to serum transferrin and cholinesterase were affected by liver dysfunction (*7*). We thus compared the serum A3G3Fo level with the glutamic oxaloacetic transaminase (GOT) and glutamic pyruvic transaminase (GPT) values of each NSCLC patient, but there were no patients who had apparent liver dysfunction (Table II).

DISCUSSION

The present report is the first description of the structures of *N*-linked oligosaccharides present in the whole human serum. We applied two-dimensional oligosaccharide analysis and determined oligosaccharide structures without the purification of glycoprotein. This method, developed primarily by the research groups of Hase (*8*) and Takahashi (*9*), has proven to be very useful in the determination of oligosaccharide structure. A general rule was also found governing the shift on the two-dimensional map by adding or reducing the residues of *N*-linked oligosaccharides. In previous studies, few reports have analyzed *N*-linked oligosaccharide structure expressed in the whole tissue without purification of glycoprotein (*10*, *11*), since structural analysis has been predominantly performed after purification of the glycoprotein (*12*, *13*). The information obtained from such studies has been limited to the *N*-linked oligosaccharide structures harbored on one glycoprotein, precluding the detection of overall changes in *N*-linked oligosaccharide structures in the whole tissue or in the entire body. Whole serum examination is thought to be much simpler and less expensive than analyses involving protein purification, and thus useful in a routine clinical examination.

N-linked oligosaccharide composition was extremely constant throughout the samples from healthy volunteers, indicating that analysis of *N*-linked oligosaccharides in human sera may be a useful tool for clinical examination. To evaluate the feasibility of serum oligosaccharide analysis, we initially analyzed sera from NSCLC patients. Although the amounts of most of the *N*-linked oligosaccharides in patient sera did not vary significantly from those in normal sera, the level of one oligosaccharide (A3G3Fo) was significantly higher in patient sera than in healthy volunteers' sera (Table I and Fig. 4). Histological type and stage of disease for NSCLC patients did not influence the distribution of A3G3Fo content (Table II). The levels of A3G3Fo in human sera exhibited little correlation with another cancer marker (SLX) or inflammation markers (WBC, CRP) (Table II). The reason for the low correlation between serum A3G3Fo and SLX level may be that most of the serum SLX is thought to be present on *O*-linked oligosaccharides, while the A3G3Fo level we measured was on *N*-linked oligosaccharides. Moreover, we have not quantified how much of the A3G3Fo had been sialylated before neuraminidase treatment.

Thus these results suggest that quantitation of the A3G3Fo content in human sera is a promising tool for early serological detection of NSCLC. The A3G3Fo content in the sera of healthy volunteers was found to be distributed within the mean ± 2SD (0–4.09). If the cut-off value is taken to be 4.09%, then 8 out of 14 samples (57.1%) from patients with NSCLC exceeded the cut-off value.

Triantennary oligosaccharide with Lewis X epitope is reported to be detected on serum glycoproteins in patients with liver dysfunction or pregnancy (*7*, *13*). But there were no patients with apparent liver dysfunction or pregnancy (Table II). Therefore, it is highly likely that A3G3Fo level is at least cancer-associated and is a novel index worthy of evaluation for the detection of NSCLC.

The level of A3G3Fo with the structure of fucoseα1→3GlcNAcβ1→4 attached to trimannosyl core was increased in the NSCLC patients, while that of A3G3 was not. This suggested that α1→3fucosyltransferase activity is up-regulated somewhere in the body of NSCLC patients. Togayachi *et al.* (*14*) recently reported that fucosyltransferase-III (FucT-III) and VI (FucT-VI) were up-regulated in NSCLC tissue in comparison to adjacent normal lung tissue. Both FucT-III and VI catalyze α1→3fucosylation, thus it is possible that A3G3Fo is increased in NSCLC tissues, which may be released into the serum. However, this is less likely because we could not detect A3G3Fo in NSCLC tissues.

Measurement of A3G3Fo levels in sera of patients carrying other cancers is necessary to determine whether the high level of serum A3G3Fo is specific to NSCLC or is generally associated with cancers. The production of monoclonal antibodies that specifically recognize A3G3Fo would simplify the assay system and ultimately facilitate the collection of additional clinical data.

We thank Dr. S. Yazawa for critical reading of the manuscript and helpful discussions and Ms. I. Itoh for her technical assistance.

REFERENCES

1. Shields, T.W. (1994) *Surgical Treatment of Non-Small Cell Bronchial Carcinoma*, pp. 1159–1187, General Thoracic Surgery 4th ed., William & Wilkins, Philadelphia
2. Fraser, R.G., Peré, J.A.P., Peré, P.D., Fraser, R.S., and Genereux, G.P. (1989) *Epidermology in Carcinoma of Airway and Alveolar Epithelium,* pp. 1329–1330, W.B. Saunders, Philadelphia
3. Fujimoto, I., Menon, K.K., Otake, Y., Tanaka, F., Wada, H., Takahashi, H., Tsuji, S., Natsuka, S., Nakakita, S., Hase, S., and Ikenaka, K. (1999) Systematic analysis of N-linked sugar chains from whole tissue employing partial automation. *Anal. Biochem.* **267**, 336–343
4. World Health Organization (1982) The World Health Organization histological typing on lung tumors. Second edition. *Am. J. Clin. Pathol.* **77**, 123–136
5. Mountain, C.F. (1997) Revision in the International System for Staging Lung Cancer. *Chest* **111**, 1710–1717
6. Satoh, H., Yano, H., Naitoh, T., Takahashi, N., Suyama, T.,

Downloaded from http://jb.oxfordjournals.org/ at Peking University on October 1, 2012

Murayama, J., Kameyama, M., Fukuda, K., Satoh, T., and Ohtsuka, M. (1988) Determination of various tumor markers, with special reference to sialyl SSEA-1 antigen in lung cancer. *Jpn. J. Cancer Chemother.* **15**, 2917–2922
7. Ohkura, T., Hada, T., Higashino, K., Ohue, T., Kochibe, N., Koide, N., and Yamashita, K. (1994) Increase of fucosylated serum cholinesterase in relation to high risk groups for hepatocellular carcinomas. *Cancer Res.* **54**, 55–61
8. Hase, S., Ikenaka, K., Mikoshiba, K., and Ikenaka, T. (1988) Analysis of tissue glycoprotein sugar chains by two-dimensional high-performance liquid chromatographic mapping. *J. Chromatogr.* **434**, 51–60
9. Tomiya, N., Awaya, J., Kurono, M., Endo, S., Arata, Y., and Takahashi, N. (1988) Analyses of N-linked oligosaccharides using a two-dimensional mapping technique. *Anal. Biochem.* **171**, 73–90
10. Chen, Y., Wing, D.R., Guile, G.R., Dwek, R.A., Harvey, D.J., and Zamze, S. (1988) Neutral N-glycans in adult rat brain: complete characterisation reveals fucosylated hybrid and complex structure. *Eur. J. Biochem.* **251**, 691–703
11. Guile, G.R., Rudd, P.M., Wing, D.R., Prime, S.B., and Dwek, R.A. (1996) A rapid high-resolution high-performance liquid chromatographic method for separating glycan mixtures and analyzing oligosaccharide profile. *Anal. Biochem.* **240**, 210–226
12. Flahaut, C., Capon, C., Balduyck, M., Ricart, G., Sautiere, P., and Mizon, J. (1998) Glycosylation pattern of human inter-α-inhibitor heavy chains. *Biochem. J.* **333**, 749–756
13. Nemansky, M., Thotakura, N.R., Lyons, C.D., Ye, S., Reinhold, B.B., Reinhold, V.N., and Blithe, D.L. (1998) Developmental changes in the glycosylation of glycoprotein hormone free a subunit during pregnancy. *J. Biol. Chem.* **273**, 12068–12076
14. Togayachi, A., Kudo, T., Ikehara, Y., Iwasaki, H., Nishihara, S., Andoh, T., Higashiyama, M., Komada, K., Nakamori, S., and Narimatsu, H. (1999) Up-regulation of Lewis enzyme (Fuc-TIII) and plasma-type α1,3fucosyltransferase (Fuc-TVI) expression of sialyl Lewis x antigen in non-small cell lung cancer. *Int. J. Cancer* **83**, 70–79

Downloaded from http://jb.oxfordjournals.org/ at Peking University on October 1, 2012